Journal of Environmental Management 197 (2017) 393–403

Contents lists available at ScienceDirect

Journal of Environmental Management

journal homepage: www.elsevier.com/locate/jenvman

Research article

Effect of the acid treatment conditions of kaolinite on etheramine adsorption: A comparative analysis using chemometric tools

Paulo Vitor Brandão Leal [a, b], Zuy Maria Magriotis [c, *], Priscila Ferreira de Sales [d], Rísia Magriotis Papini [e], Paulo Roberto de Magalhães Viana [e]

[a] Colegiado do Bacharelado em Ciências e Tecnologia da Universidade Federal dos Vales do Jequitinhonha e Mucuri, 39.440-000, Janaúba, MG, Brazil
[b] Departamento de Química, Universidade Federal de Lavras, 37200-000, Lavras, MG, Brazil
[c] Departamento de Engenharia, Universidade Federal de Lavras, 37200-000, Lavras, MG, Brazil
[d] Instituto Federal de Educação Ciência e Tecnologia de Minas Gerais - Campus Bambuí, 38900-000, Bambui, MG, Brazil
[e] Departamento de Engenharia de Minas, Universidade Federal de Minas Gerais, 31270-901, Belo Horizonte, MG, Brazil

ARTICLE INFO

Article history:
Received 26 June 2016
Received in revised form
28 March 2017
Accepted 1 April 2017
Available online 12 April 2017

Keywords:
Acid treatment
Kaolinite
Response surface methodology
Etheramine
Mining effluents

ABSTRACT

The present work evaluated the effect of the acid treatment conditions of natural kaolinite (NK) regarding its efficiency in removing etheramine. The treatment was conducted using sulfuric acid at the concentrations of 1 mol L^{-1} (KA-01), 2 mol L^{-1} (KA-02) and 5 mol L^{-1} (KA-05) at 85 °C. The obtained adsorbents were characterized by X-ray fluorescence, X-ray diffraction, N_2 adsorption/desorption isotherms, zeta potential analysis and infrared spectroscopy. The Response Surface Method was used to optimize adsorption parameters (initial concentration of etheramine, adsorbent mass and pH of the solution). The results, described by means of a central composite design, were adjusted to the quadratic model. Results revealed that the adsorption was more efficient at the etheramine concentration of 400 mg L^{-1}, pH 10 and adsorbent mass of 0.1 g for NK and 0.2 g for KA-01, KA-02 and KA-05. The sample KA-02 presented a significant increase of etheramine removal compared to the NK sample. The adsorption kinetics conducted under optimized conditions showed that the system reached the equilibrium in approximately 30 min. The kinetic data were better adjusted to the pseudo-second order model. The isotherm data revealed that the Sips model was the most adequate one. The calculation of E_{ads} allowed to infer that the mechanism for etheramine removal in all the evaluated samples was chemisorption. The reuse tests showed that, after four uses, the efficiency of adsorbents in removing etheramine did not suffer significant modifications, which makes the use of kaolinite to treat effluents from the reverse flotation of iron ore feasible.

1. Introduction

In the past years, the mining activity has led to studies on its sustainability due to the concern about environmental and social issues that surround this industry in the world. These studies have been increasingly focused on the need for a modern mining model inserted in a more sustainable context in which annual reports of companies relate not only their financial results, but also their performance regarding the sustainable use of resources (Mudd, 2010). In this sense, the use of water resources stands out once, during the mining process, the activities linked to ore beneficiation consume an expressive amount of water. Among such activities, flotation is the most widely used step for ore concentration, which consumes approximately 5 m^3 h^{-1} of water per ton of processed ore. Moreover, it uses different chemical reagents to make the process feasible (Magriotis et al., 2010).

Flotation is the most effective solution, from both a technological and economical point of view, for the beneficiation of iron ore. Research on this method started in 1931 demonstrating that reverse cationic flotation is an efficient method for the beneficiation of oxidized iron ore. Flotation may also be applied to reduce the silica content in magnetite concentrate (Filippov et al., 2014). Despite the high applicability to the industry of iron ore, it is verified that this ore beneficiation step presents some problems associated with the great metal waste and high costs of amine

* Corresponding author.
E-mail addresses: paulo.leal@ufvjm.edu.br (P.V.B. Leal), zuy@deg.ufla.br (Z.M. Magriotis), priscila.sales@ifmg.edu.br (P.F. Sales), risia@demin.ufmg.br (R.M. Papini), pviana@demin.ufmg.br (P.R.M. Viana).

http://dx.doi.org/10.1016/j.jenvman.2017.04.003
0301-4797/

collectors (Ma et al., 2011). It is important to highlight that the etheramine applied as cationic collector in the process of reverse flotation of iron ore is discarded in tailings dams, which requires the search for alternatives to recover this reagent (Araújo et al., 2010).

The degradation of etheramine, a reagent used in the reverse flotation of iron ore, occurs by the action of microorganisms, which happens in approximately 28 days. However, with the continuous process of sedimentation, this degradation may be insufficient leading to the contamination of watercourse. This reagent is corrosive, very toxic to aquatic organisms and has a high value of chemical oxygen demand (Magriotis et al., 2010). This fact shows the importance to reuse part of this reagent because of economical or environmental aspects. Therefore, adsorption can be an interesting alternative for the treatment of this effluent.

Adsorption has been considered one of the most efficient and economical processes for the removal of pollutants from water, which stands out due to its low cost and operational limits (Poonkuzhali et al., 2014). Among a great variety of adsorbents that can be used, clay minerals have been used as an alternative to make adsorption feasible for different processes.

Kaolinite ($Al_2Si_2O_5(OH)_4$) is defined as a clay-mineral type 1:1, consisting of two basic units. The first consists of an octahedral layer composed by oxygen atoms and hydroxyl groups in a compact way, in which atoms of aluminum, iron and magnesium are arranged in this coordination. The second is called tetrahedral unit of silica in which the silicon atom in the center is equidistant from four oxygen atoms or possibly hydroxyls (Morsy et al., 2014).

Clay minerals are low-cost, abundant and generally safe materials for environmental applications due to the possibility of having different characteristics such as high porosity, surface charge and surface functional groups. They can be used as adsorbents, filters, flocculators and carbon stabilizers. Moreover, their physicochemical and mechanical properties allow structural, textural and chemical changes, which makes them good adsorbents and carriers of organic compounds (Perez et al., 2014; Yuan et al., 2013).

During acid activation, exchangeable cations of the clay are replaced by H^+ ions from the acid, causing partial modifications to the crystalline structure of the acidified material. The effect of such modification contributes to the increase in surface acidity, surface area and porosity. The material resulting from the acid treatment consists of one part of the starting mineral and the other of a porous, protonated and hydrated amorphous silica phase with a three-dimensional cross-linked structure (Ugochukwu et al., 2014); (Komadel and Madejová, 2012).

There are two ways one can investigate the effect of a large number of variables. The most commonly used method involves the variation of one variable, while keeping the other variables constant, until all variables have been studied. This methodology has two disadvantages: first, a large number of experiments are required, and second, it is likely that the combined effect of two or more variables may not be identified (Frontistis et al., 2017). One way to avoid these flaws is to consider a statistical approach with an experimental design.

Chemometric tools have been frequently applied to methods to optimize analysis as they reduce the number of required experiments, among other advantages that result in a lower consumption of reagents and duration of experiments These tools allow the simultaneous study of several control parameters and the development of mathematical models to evaluate the relevance and significance of the studied parameters. Furthermore, they facilitate the evaluation of interactions among parameters. There are two types of variables in multivariate projects: (i) qualitative and quantitative responses and (ii) factors, which can be selected by fractional or complete factorials to obtain results of significant effects over the analytical response (Tarley et al., 2009; Asadollahzadeh et al., 2014).

The optimization through the factorial design and response surface analysis is largely applicable. For adsorption, the application of a statistical experimental design may increase product yield and reduce the variability, costs and duration of the process (Chatterjee et al., 2012). Therefore, research has been conducted in order to combine factorial design and response surface to optimize the removal of contaminants of distinct classes that include dies (Chatterjee et al., 2012; Ravikumar et al., 2006; Sales et al., 2013; Singh et al., 2011) and heavy metals (Garg et al., 2008; Kavalathy et al., 2009).

In this context, the present work aimed to investigate the influence of chemical treatment on the adsorption capacity of etheramine by kaolinite using the Response Surface approach for the optimization of parameters of the adsorption process (initial concentration of adsorbate, adsorbent mass and pH of solution).

2. Materials and methods

2.1. Adsorbate

For the tests of adsorption, solutions of amine Flotigan EDA - etheramine acetate with dodecyl radical neutralized at 30% (Clariant) - from a storage solution with concentration of 2 g L^{-1} were prepared.

2.2. Adsorbent

The *in natura* kaolinite used as adsorbent and matrix for the chemical treatments was provided by Mineradora Química e Minérios from the city of Ijaci in the state of Minas Gerais, Brazil. For the adsorption tests, kaolinite was crushed and sieved through a 0.42 mm mesh (35 Tyler).

2.3. Modification of kaolinite by acid treatment

The acid treatments were performed with solutions of sulfuric acid at different concentrations (1 mol L^{-1}, 2 mol L^{-1} and 5 mol L^{-1}) under reflux at 85 °C and agitation, for 3 h. After the treatment, the samples were filtered with deionized water until neutral pH and dried in a lab oven at 100 °C for 2 h. The samples KA-01, KA-02 and KA-05 were crushed and sieved through a 0.42 mm mesh (35 Tyler).

2.4. Characterization of adsorbents

The chemical composition of the adsorbents was determined by X-ray fluorescence (Phillips CUBIX 3600). The XRD analyses were conducted in a spectrophotometer, model Philips PW1710, using CuKα_1 radiation with scan of 4° and 9° (2θ) and scan rate of 0.6°θ s^{-1}. The specific surface area of adsorbents was determined through the measurement of adsorption and desorption of nitrogen at −196 °C with the Brunauer-Emmett-Teller method (BET) in a Micrometrics ASAP 2020. To determine the zeta potential, suspensions of the adsorbent (particle size < 37 μm) were deposited/conditioned in bottles at 22 °C during 2 h at pH from 2 to 12 with a solution of 2 mmol L^{-1} of sodium nitrate as supporting electrolyte. The measurements of potentials were conducted in a Zeta Meter model ZM3-DG, in which the applied tension ranged from 75 to 200 mV. The infrared spectra were obtained from an ATR analysis (Attenuated Total Reflectance) with an interval from 4000 to 400 cm^{-1}, resolution of 4 cm^{-1} and 64 scans in a Bruker Vertex70V series spectrometer.

2.5. Experimental design

In order to optimize the analysis of adsorption of etheramine in modified kaolinite, an experimental design was proposed, in which the parameters: initial concentration, adsorbent mass and pH of the solution were studied through a Central Composite Design (CCD). In this design, n represents the number of experiments consisting of 2^n factorial points, 2n axial points and three central points, in which n represents the number of independent variables. Since the study evaluated three variables, the experimental design involved 17 trials. The Chemoface 1.4 software (Nunes et al., 2012) was used to delineate and define the best conditions of adsorption by estimating statistical parameters.

2.6. Adsorption experiments

The adsorption tests were conducted with the proposed factorial design. For this purpose, aliquots of 10 mL of solutions of etheramine of known concentrations, and pH adjusted with 0.1 mol L^{-1} KOH solution (for basic solutions) and glacial acetic acid (for acid solutions), were put together with the adsorbents in pre-established amounts and kept under agitation at 200 rpm, temperature of 25 °C during 24 h in an Incubator Shaker (ACB Labor).

After agitation, the solutions were filtered and the supernatants were collected and quantified through the Bromocresol Green method (Magriotis et al., 2010). The concentration of etheramine remaining from the adsorption process was determined with a UV–vis spectrophotometer (Femto, model 800 XI) with wave length of 410 nm. The experiments were performed in duplicates. The percentage of etheramine removal was defined based on equation (1):

$$\%R = \frac{C_i - C_t}{C_i} \times 100 \quad (1)$$

where C_i is the initial concentration of etheramine (mg L^{-1}) and C_t is the concentration of etheramine (mg L^{-1}) at time t.

2.7. Adsorption kinetics

In order to define the time at which equilibrium was reached, adsorption tests were performed under optimized conditions during a time interval from 5 min to 24 h.

2.8. Adsorption isotherms

The adsorption isotherms were evaluated from the optimization and determination of the time at which equilibrium was reached. Solutions of etheramine were prepared at the concentrations of 10, 30, 50, 100, 250, 400, 500, 1000 and 2000 mg L^{-1}. The amount of etheramine adsorbed at equilibrium (Q_e mg g^{-1}) was determined by equation (2):

$$Q_e = \frac{(C_i - C_e)V}{m} \quad (2)$$

where C_i is the initial concentration of etheramine (mg L^{-1}), C_e is the concentration of etheramine at equilibrium (mg L^{-1}), m is the mass of adsorbent (g) and V the volume of solution (L).

2.9. Reuse tests

After the tests of adsorption, kaolinite samples were washed with deionized water (20 mL of water per gram of adsorbent) at 60 °C for 2 h. The material was filtered and dried in a lab oven at 100 °C during 16 h. The adsorbents, after desorption, were reused in the process of etheramine adsorption under the optimized conditions. The reuse process was repeated three times for each adsorbent.

3. Results and discussion

3.1. Characterization of adsorbent

The XRF analysis was used to determine the chemical composition of the samples, as well as to verify the chemical changes that occurred due to the acid treatment. The results are shown in Table 1.

The samples consist mainly of silicon and aluminum oxides, which are characteristic of clay minerals. Lower amounts of oxides of sodium, potassium, iron and magnesium were verified. It was also observed that, as the concentration of the acid increased, the content of Al_2O_3 and Fe_2O_3 decreased gradually. The reaction between kaolinite and sulfuric acid may be described by equation (3):

$$Al_2O_3 \cdot 2SiO_2 \cdot 2H_2O_{(s)} + 3H_2SO_{4\ (aq)} \rightarrow Al_2(SO_4)_{3\ (aq)} + 2\ SiO_{2(s)} + 5H_2O_{(l)} \quad (3)$$

Equation (3) shows that the increase in the Si/Al ratio is possibly attributed to the leaching of Al^{3+} ions from the octahedral layers during hydrolysis under acid conditions. Meanwhile, the decrease in iron oxide content is associated with its dissolution by sulfuric acid during the treatment. The decrease in MgO content after kaolinite was submitted to the three treatments is possibly related to the substitution of cations of alkaline earth metals present in the crystalline structure or exchangeable cations for H_3O^+ ions (Cristóbal et al., 2009).

The score chart (Fig. 1S) showed that the two first main components explained, jointly, 100% of the data variability, from which 99.89% was explained by the first main component (PC1) and 0.11% by the second (PC2). This chart shows the separation of samples submitted to acid treatment, among which the sample KA-05 was the most distinct, especially when compared with NK.

The joint assessment of score graphs (Fig. 1S) and weight (Fig. 2S) reveals that the contents of Al_2O_3 and SiO_2 are mainly responsible for the separation of samples. This confirms the efficiency of the acid treatment on changing the main components of the starting material, which is consistent with results already reported in the literature (Dudkin, 2010). It can also be observed that the NK sample stands out due to the greater amount of Al_2O_3, while the KA-05 sample stands out because of the higher content of SiO_2. This result may be associated with the increase in the intensity of dealumination as the concentration of the acid increased, thus leading to the formation of a material with high content of silica (Dudkin, 2010).

According to the results from the analysis of auto-scaled components of samples, a dendrogram was obtained (Fig. 3S), where samples were organized on the X-axis, and the similarity index was organized on the Y-axis, and samples were included as a function of their similarity. The acid treatment which least modified the chemical composition of kaolinite was the one conducted with the

Table 1
Chemical composition of the kaolinite samples.

Sample	SiO_2	Al_2O_3	Fe_2O_3	MgO	Na_2O	K_2O
NK	52.75	43.13	3.05	0.46	0.09	0.52
KA-01	53.72	42.68	2.76	0.09	0.23	0.52
KA-02	54.98	41.52	2.65	0.07	0.24	0.54
KA-05	57.35	39.27	2.54	0.08	0.23	0.53

concentration of 1 mol L^{-1}, whereas the treatment with a concentration of 5 mol L^{-1} was the one that modified the chemical composition of NK the most. It can be inferred that the increase in acid concentration led to the increased leaching process, which, in turn, alters the two main constituents of the clay minerals, silica and alumina.

The XRD results (Fig. 1) show that the adsorbents have some impurities (a fraction of quartz). The diffractogram of chemical treatments did not show significant changes when compared to the NK one. Thus, the structure of kaolinite was preserved after the acid treatment. Similar results are found in the literature (Melo et al., 2010).

The surface charge of adsorbents was evaluated according to the variation of pH. Results are shown in Fig. 2. It is possible to observe that the treatment conducted with the lowest acid concentration (KA-01) was more similar to the tendency observed for the NK sample, and the isoelectric point was the closest point to the starting material. Therefore, it is possible to infer that the acid concentration used did not act in the complete substitution of exchangeable cations of the NK sample for H^+ ions.

KA-02 and KA-05 showed lower values of isoelectric point when compared to the NK and KA-01samples, thus highlighting a greater positive surface character. Such fact is related to the more drastic conditions of treatment, which cause a greater leaching effect of Al^{3+} ions from the octahedral layers during hydrolysis and substitution of exchangeable cations for H^+ ions.

The textural properties of adsorbents are presented in Table 2. The natural kaolinite (NK) presented a surface area of 33.5 m^2g^{-1}. The value found is within the range found in the literature (8.08–35.3 m^2g^{-1}) (Chen and Lu, 2015; Khawmee et al., 2013; Melo et al., 2010; Ndlovu et al., 2015; Panda et al., 2010; Xu et al., 2015; Wei et al., 2014). The differences observed for values of surface area may be justified by the distinct chemical composition or crystallinity shown by the kaolinites, once they came from different regions.

Acid treatments led to an increase in the surface area of kaolinite, and, in this matter, the sample KA-02 stands out (Table 2). These results suggest that such treatments effectively improved the textural properties of kaolinite, which is possibly attributed to the dissolution of metal ions present in the NK sample and the rearrangement of its crystalline structure resulting from the reaction between the acid and clay minerals. This is corroborated by other studies reported in the literature (Chen and Lu, 2015; Panda et al., 2010). The decrease in surface area when the concentration 5 mol L^{-1} (KA-05) was applied may be associated with the more drastic conditions of treatment.

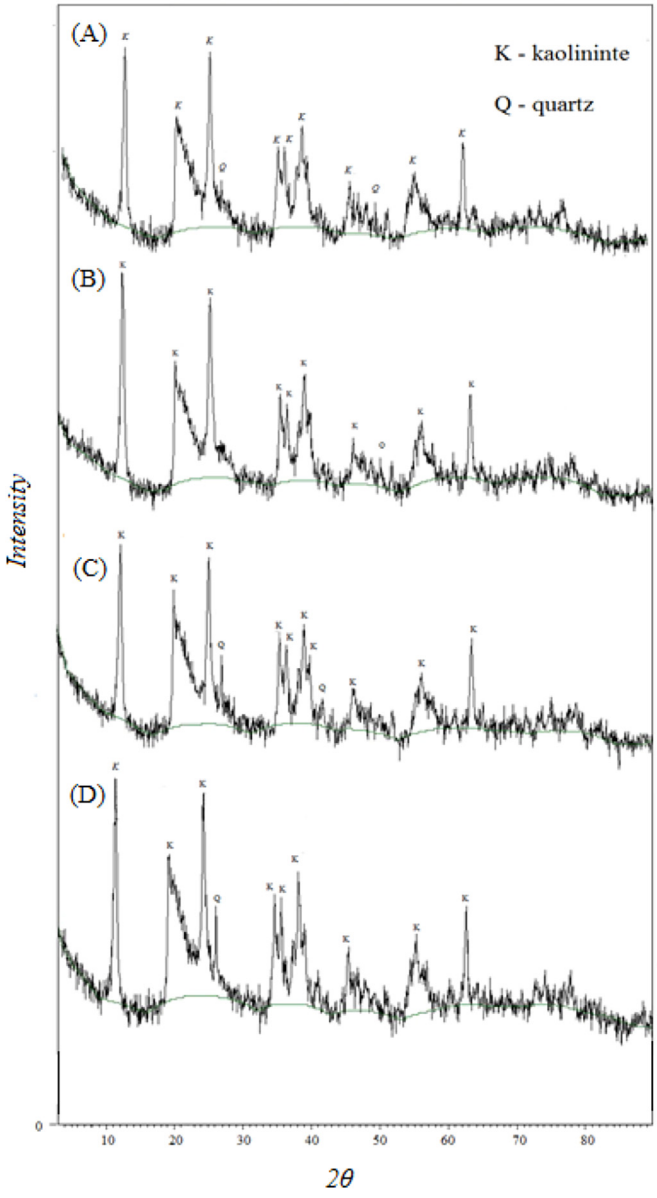

Fig. 1. Analysis of X-Ray diffraction (XRD) of NK (A), KA-01 (B), KA-02 (C) and KA-05 (D).

3.2. Optimization of the adsorption parameters

The optimization through Response Surface (in duplicates) as well as the mean values of percentage of etheramine removal are shown in Table 3 and Table 4.

The Pareto chart may be defined as a statistical tool that allows a clear visualization of the effect of variables (Nunes et al., 2012). The results obtained for the adsorption of etheramine in the modified kaolinite are shown in Fig. 4S. It was possible to observe that the acid treatments applied to kaolinite affected the influential variables in the etheramine adsorption significantly.

Among the studied parameters, pH showed a higher influence on adsorption, which is related to the alteration of the etheramine forms and of the surface charge of modified kaolinite as the pH was altered. It was also possible to observe a positive effect in all cases, which indicates that the increased pH contributes to the increase in etheramine adsorption. This result may be related to the modification of the surface charge of kaolinite that tends to become negative in basic medium. Such factor favors the mechanism of electrostatic attraction among the positively charged molecules of etheramine in the ionic form and the negative surface of the adsorbent.

Another important factor was the increase in the significance level of the adsorbent mass in the adsorption of modified kaolinites, once for the natural kaolinite this parameter was not influenced. This variable has a positive effect, meaning a directly proportional relationship with the removal percentage.

The Pareto chart showed that, in more drastic acid treatments (KA-02 and KA-05), the initial concentration became significant and presented a positive effect directly proportional to the removal percentage. These facts suggest that the different treatments applied to kaolinite had a significant effect on the adsorption process, and the combined parameters were very susceptible to be influenced in the studied process.

In order to determine the more adequate conditions for the

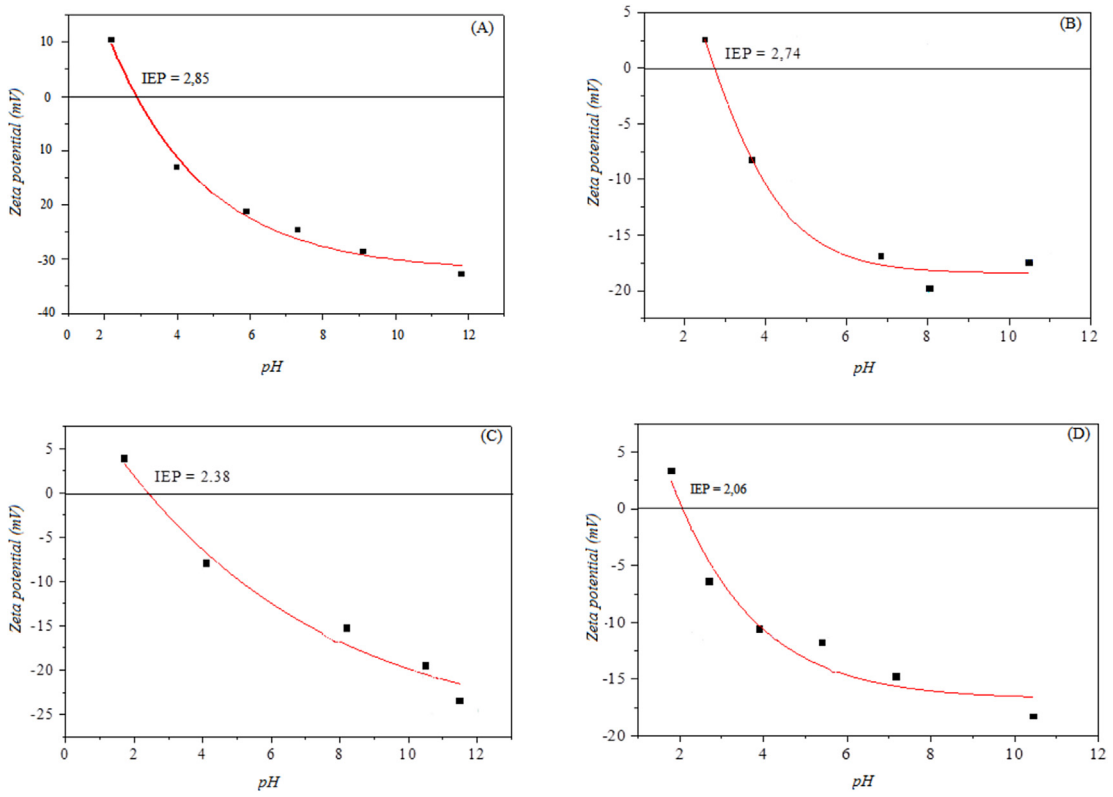

Fig. 2. Influence of pH on zeta potential in NK (A), KA-01 (B), KA-02 (C) and KA-05 (D).

Table 2
Textural properties of the adsorbents.

Samples	Specific surface area ($m^2\ g^{-1}$)	Pores volume ($cm^3\ g^{-1}$)	Average pore diameter BJH(Å)
NK	33.5	0.18	36.7
KA-01	40.8	0.19	37.1
KA-02	50.2	0.20	37.5
KA-05	45.1	0.19	37.2

Table 3
Independent variables of the central composite design.

	Initial concentration of etheramine (mg L^{-1})	Mass of adsorbent (g)	pH
–	100	0.050	4
+	400	0.200	10
BM	10	0.001	2
AM	500	0.251	12
CP	250	0.125	7

* BM: Below the minimum; AM: above the maximum; CP: Central point.

process of adsorption, the system was optimized by the application of the Response Surface Methodology. The quality of the data adjustment was evaluated according to the analysis of variance.

Based on the variables and interactions which are statistically significant to the quadratic model, a model describing the experimental response was built, considering the following equations for the adsorbents: NK, KA-01, KA-02 and KA-05, respectively. In the equations, X_1, X_2 and X_3 represent, respectively, the initial concentration of etheramine (mg L^{-1}), mass of adsorbent (g) and pH.

$$y = -33.45 + 12.66X_3 - 0.01X_1X_3 - 17.63X_2X_3 + 1.79x10^{-4}X_1^2 + 347.78X_2^2 \quad (4)$$

$$y = -69.51 + 0.30X_1 + 11.40X_3 - 0.015X_1X_3 + 25.44X_2X_3 - 3.85x10^{-4}X_1^2 - 524.99X_2^2 - 0.28X_3^2 \quad (5)$$

$$y = -33.88 + 0.12X_1 + 230.48X_2 + 3.30X_3 - 0.27X_1X_2 + 0.01X_1X_3 + 13.87X_2X_3 - 2.21x10^{-4}X_1^2 - 560.54X_2^2 \quad (6)$$

$$y = -51.68 + 160.81X_2 + 15.73X_3 + 0.01X_1X_3 - 591.13.87X_2^2 - 1.04X_3^2 \quad (7)$$

Adequacy of the model was also checked by means of building the normal plot of the residuals (Fig. 5S). The figure reveals that the points of the KA-01 and KA-05 samples were closer to the line of tendency than the other samples. However, it is possible to observe that the quadratic model may be applied and evaluated in the range in which the parameters were studied.

The Response Surface graphs were built considering the significant interactions corresponding to the adsorbent mass, pH and initial concentration of etheramine. The effect of the interaction between the adsorbent mass and pH with initial concentration maintained at 250 mg L^{-1} is shown in Fig. 3.

It was possible to observe that the maximum adsorption occurred in basic medium, both for natural and modified kaolinite, in which pH = 10 stands out since it represents the moment when adsorption may be improved by the formation of an ionic-molecular complex of etheramine (Magriotis et al., 2013). Therefore, adsorption may be considered a feasible process in the

Table 4
Matrix with results of the etheramine adsorption.

Assay	Initial concentration of etheramine (mg L^{-1})	Mass of adsorbent (g)	pH	Adsorption of etheramine (%)			
				NK	KA-01	KA-02	KA-05
1	−	−	−	0.40	5.22	12.76	12.10
2	−	−	+	63.00	64.85	52.10	48.56
3	−	+	−	5.57	1.67	21.95	14.59
4	−	+	+	36.63	88.14	84.21	52.12
5	+	−	−	11.12	4.78	3.53	1.80
6	+	−	+	43.93	41.96	66.06	51.15
7	+	+	−	5.00	0.1	11.00	0.71
8	+	+	+	37.62	56.23	75.57	63.40
9	BM	CP	CP	20.71	0.1	0.20	2.90
10	AM	CP	CP	28.90	27.26	37.38	51.22
11	CP	BM	CP	11.71	8.93	4.76	3.81
12	CP	AM	CP	26.13	50.67	43.10	44.17
13	CP	CP	BM	5.65	16.43	14.52	2.94
14	CP	CP	AM	4.13	45.83	52.38	11.15
15	CP	CP	CP	20.51	42.98	44.40	42.26
16	CP	CP	CP	18.01	45.12	43.60	42.38
17	CP	CP	CP	19.33	43.60	41.82	39.16

treatment of mining effluents, since, at such pH value, the reverse flotation of iron ore occurred. In relation to the adsorbent mass, it was possible to verify that for NK the maximum adsorption occurred for the mass of 0.1 g, while for the modified kaolinites the higher removal percentages occurred with mass next to 0.2 g. The significant influence of this parameter is associated to the increased number of available adsorption sites.

The effect of the interaction between the initial concentration and pH with the mass of 0.125 g corresponding to the central point is shown in Fig. 4.

The higher percentage of etheramine removal is optimized at more elevated concentrations, next to 400 mg L^{-1}, which can be attributed to the existence of more adsorbate molecules interacting with the surface of the adsorbent material. Thus, it is possible to infer that the two combined parameters were influenced in the process for all adsorbents and that the basic medium was the most adequate for the adsorption process.

The effect of the interaction between the initial concentration and adsorbent mass with pH 7 corresponding to the central point is shown in Fig. 5.

It is observed that the interaction of adsorbent mass and the initial concentration when pH was kept constant resulted in the

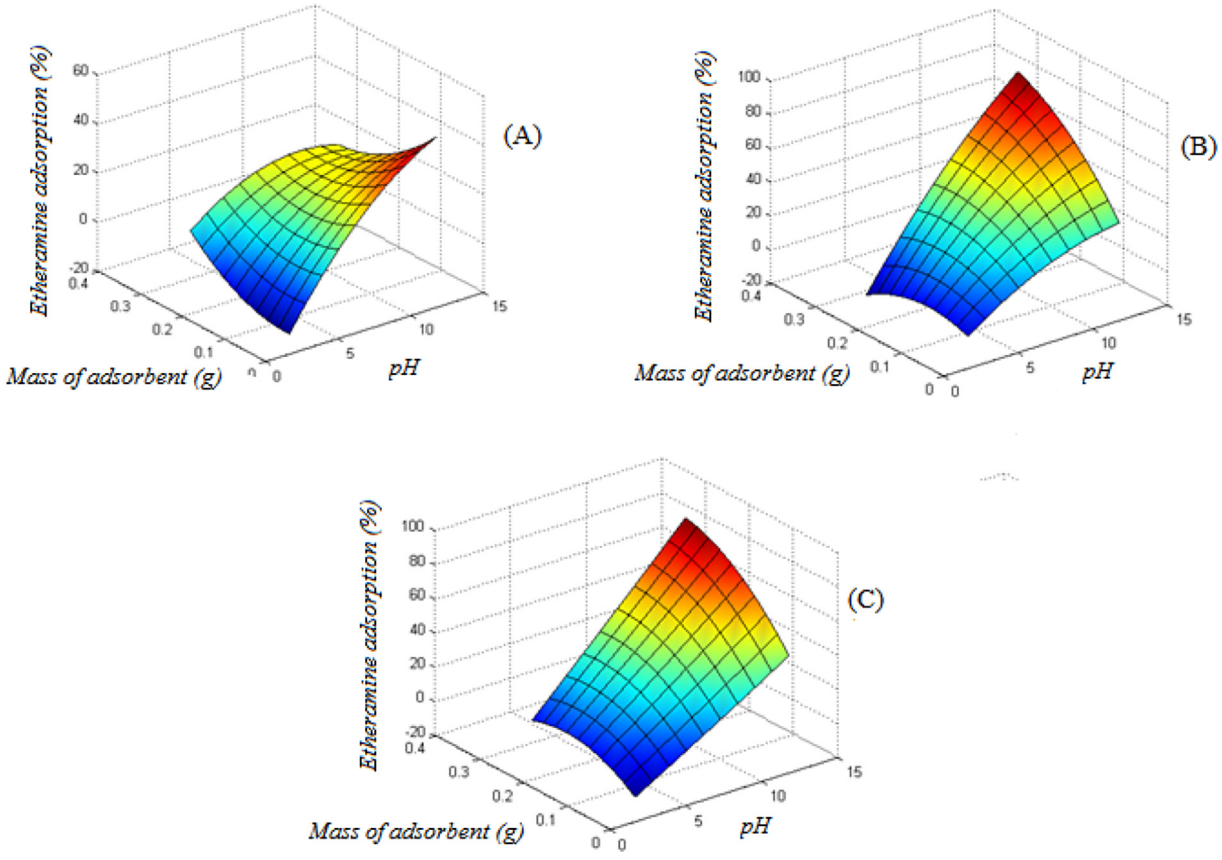

Fig. 3. Response Surface Analysis of the adsorption capacity *versus* effect of the adsorbent mass and pH on the etheramine adsorption on NK (A); KA-01 (B), KA-02 (C).

least significant interaction for KA-02, and was not significant for the other adsorbents. Then, it is possible to infer that, when these two parameters are combined, the adsorption is more dependent on the interactions between the ionic-molecular complex of etheramine and the adsorbent surface than on the availability of adsorption sites (Magriotis et al., 2013).

The following optimized results were obtained: initial concentration of approximately 400 mg L^{-1}, pH = 10 and mass of 0.1 g for NK and 0.2 g for the modified kaolinites. The values found for NK are similar to those found in previous works in which the parameters were evaluated individually (Magriotis et al., 2010). It is possible to observe that the analysis of response surface is a rapid and efficient technique, besides the fact that it takes the interactions among variables into account, which does not occur in the individual analysis.

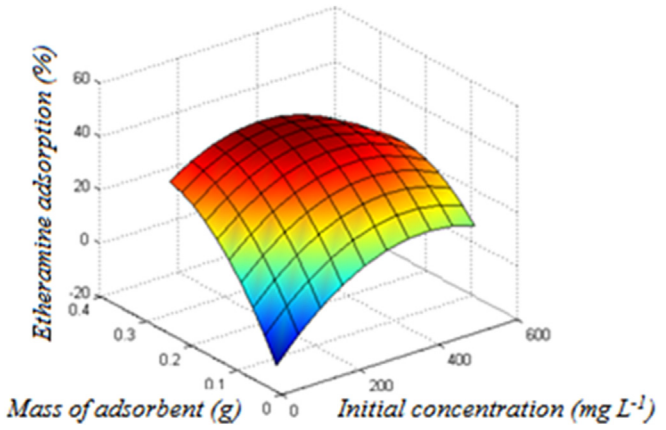

Fig. 5. Response Surface Analysis of the adsorption capacity *versus* the effect of the initial concentration and the adsorbent mass on the etheramine adsorption in KA-02.

3.3. Adsorption kinetics

An adsorption kinetic of 24 h was conducted with the optimized results in order to determine the time at which equilibrium was reached. The experiments were carried out in intervals from 5 min to 24 h (Fig. 6S). Equilibrium was reached at approximately 30 min. Subsequent analyses were performed considering a period of 2 h in order to ensure that equilibrium had already been reached.

Fig. 6 shows a comparative analysis of etheramine removal by the analyzed adsorbents using previously optimized parameters and time of equilibrium of 2 h. The removal rate was of approximately 78% for NK, 81% for KA-01, 83% for KA-05 and 88% for KA-02, and from these results, it was possible to observe that the treatments improved the efficiency of etheramine removal. The difference in removal rate is related to the specific surface area: higher removal values for the samples KA-05 and KA-02, which represent the larger surface areas corresponding to 45.13 m^2g^{-1} and 50.18 m^2g^{-1}, respectively.

3.4. Kinetic models

Adsorption may be described by different mechanisms, among which are the models of pseudo-first order (Lagergren, 1898), pseudo-second order (Ho and Mckay, 1999), Elovich (Hammed et al., 2008) and Avrami (Vargas et al., 2012), whose non-linear equations are described from (8) to (11), respectively. The data were adjusted for these models.

$$Qt = Qe[1 - \exp(-k1t)] \tag{8}$$

$$Qt = \frac{k2Q_e^2 t}{1 + Qetk2} \tag{9}$$

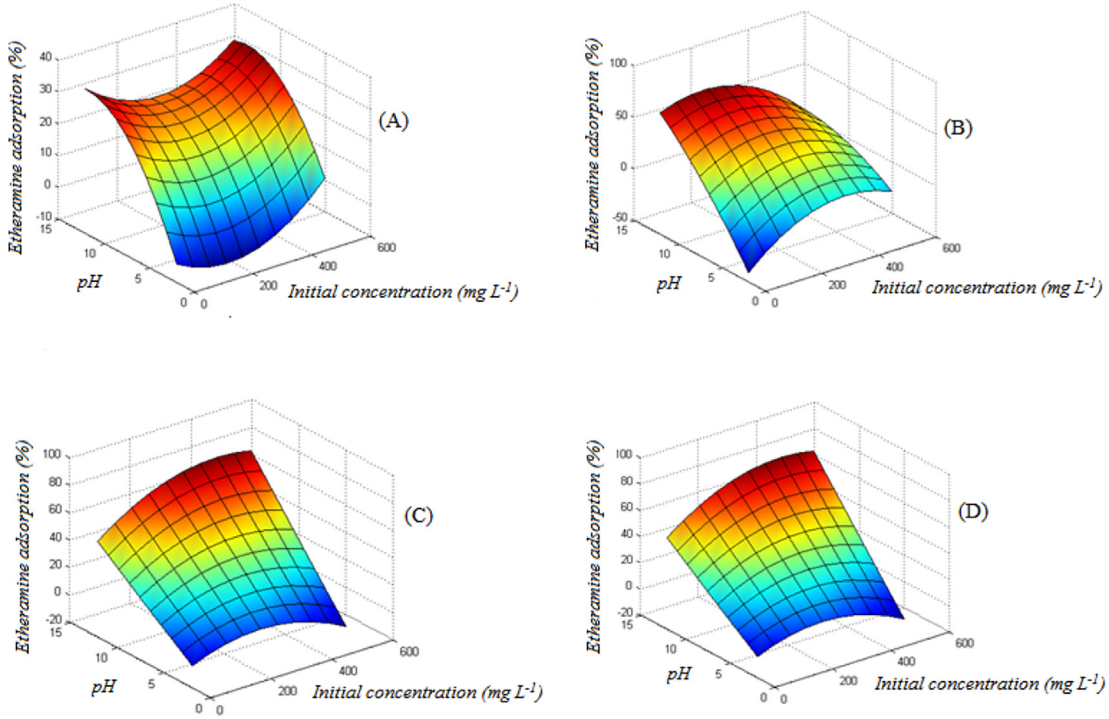

Fig. 4. Response Surface Analysis of the adsorption capacity *versus* effect of the initial concentration and pH on the etheramine adsorption on NK (A), KA-01 (B), KA-02 (C) and KA-05 (D).

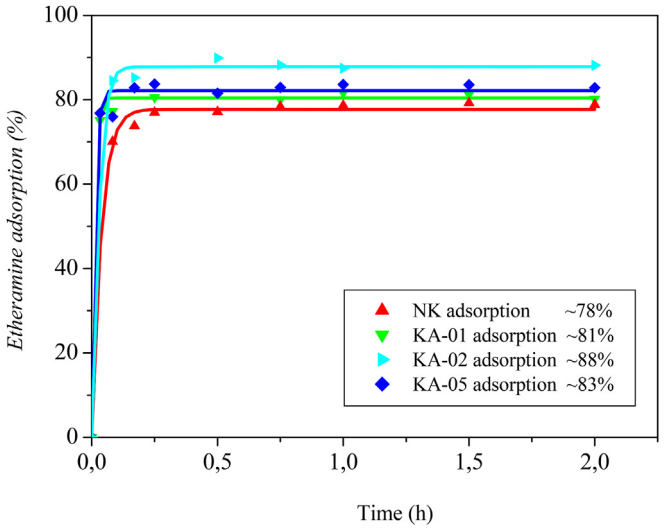

Fig. 6. Comparison of etheramine removal in the different adsorbents.

$$Q_t = \frac{1}{\beta}\ln(1 + \alpha\beta.t) \quad (10)$$

$$Q_t = Q_e\{1 - \exp[-(k_{AV}t)]^{n_{AV}}\} \quad (11)$$

where Q_t (mg g^{-1}) is the amount of etheramine adsorbed by adsorbent mass at the time t (min); Q_e (mg g^{-1}) is the amount of etheramine adsorbed by adsorbent mass at equilibrium; k_1 (min^{-1}) is the rate constant of pseudo-first order; k_2 (mg^{-1} g min^{-1}) is the rate constant of pseudo-second order; α (mg g^{-1} min^{-1}) is the rate of initial adsorption; β is the desorption constant (g mg^{-1}); k_{AV} (min^{-1}) is the kinetic constant of Avrami and n_{AV} is a constant related to the mechanism of adsorption.

The results of data adjusted to the proposed models are shown in Table 5.

Data were adjusted to the kinetic model of pseudo-second order for all the applied adsorbents. Such adjustment shows that the limiting step of adsorption is the process that happens on the surface, which is dependent on the adsorption sites, and indicates the chemical nature of adsorption (Magriotis et al., 2010).

The adjustment of the pseudo-second order kinetic model is related to the evaluation of the coefficient of determination (R^2) and average relative error (ARE), in which the R^2 values closer to 1 and lower values of ARE indicate better results. In this sense, the choice of the pseudo-second order model is related to the comparison of such parameters according to what was described in Table 5.

3.5. Adsorption isotherms

The data obtained in the experiments were adjusted to the isotherm models of Langmuir, Freundlich, Sips, Jovanovich, Redlich-Peterson and Dubinin-Radushevich. The non-linear equations are described, respectively, in (12)–(17) and the results are presented in Table 6.

$$Q_e = \frac{Q_m K_L C_e}{1 + K_L C_e} \quad (12)$$

$$Q_e = K_F C_e^{1/n} \quad (13)$$

$$Q_e = \frac{Q_m (K_s C_e)^{1/m}}{1 + (K_s C_e)^{1/m}} \quad (14)$$

$$Q_e = \frac{ARPC_e}{1 + BRPC_e^g} \quad (15)$$

$$Q_e = Q_m\left[1 - \exp(-K_J C_e)\right] \quad (16)$$

$$Q_e = Q_m e^{-b_{DR}\varepsilon^2} \quad (17)$$

$$\varepsilon = \mathrm{RTln}\,(1 + 1/\mathrm{C_e}) \quad (18)$$

where: Q_e = amount of adsorbate adsorbed per unit mass of adsorbent at equilibrium (mg g^{-1}); Q_m = capacity of monolayer coverage (mg g^{-1}); K_L = Langmuir constant (L mg^{-1}); C_e = equilibrium concentration (mg L^{-1}); K_F = Freundlich constant ($mg^{l-1/n}$ kg^{-1} $L^{1/n}$); n = parameter relating to Freundlich isotherm; K_S = Sips constant (L mg^{-1}); m = affinity distribution; ARP = Redlich-Peterson constant (L mg^{-1}); BRP = affinity coefficient (L mg^{-1}); g = heterogeneity parameter; K_J = Jovanovich constant (L mg^{-1}); b_{DR} = constant related to the energy of adsorption (mol^2 kJ^{-2}); ε = Polanyi potential; R = gas constant (kJ K^{-1} mol^{-1}); T = temperature (K).

Table 5
Adjustment of experimental data to the kinetic models.

Kinetic model		NK	KA-01	KA-02	KA-05
Pseudo-first order	Q_e (mg g^{-1})	32.2415	32.2889	35.8381	33.0683
	k_1 (min^{-1})	0.4352	1.3386	0.7749	1.3108
	R^2	0.9841	0.9956	0.9881	0.9916
	ARE	0.3231	0.1500	0.3035	0.1919
Pseudo-second ordem	Q_e (mg g^{-1})	32.9395	32.4704	36.0813	33.3979
	k_2 (g $mg^{-1}min^{-1}$)	0.0357	0.2061	0.1309	0.1402
	R^2	0.9904	0.9958	0.9893	0.9959
	ARE	0.1522	0.1536	0.2790	0.1533
Elovich	α (mg g^{-1} min^{-1})	2.98×10^9	3.36×10^9	4.14×10^9	3.14×10^9
	β (g mg^{-1})	0.6795	0.6715	0.6128	0.6522
	R^2	0.9752	0.9121	0.9470	0.9410
	ARE	0.4059	0.8329	0.622	0.6755
Avrami	k_{AV} (min^{-1})	11.5884	5.734	17.2787	23.4900
	n_{AV}	2.2532	14.01	2.6909	3.348
	R^2	0.9840	0.9956	0.9881	0.9916
	ARE	0.3223	0.7541	0.5312	0.3564

R^2 – Determination coefficient; ARE – Average relative error.

Table 6
Adjustment of experimental data to the isotherm models.

Isotherm model		NK	KA-01	KA-02	KA-05
Langmuir	Q_m (mg g^{-1})	39.95	46.99	52.57	47.87
	K_L (L mg^{-1})	0.0232	0.0327	0.0496	0.0326
	R^2	0.9281	0.9172	0.8817	0.8695
	ARE	2.2014	11.9387	8.8392	5.3803
Freundlich	K_F ($mg^{1-1/n}$ kg^{-1} $L^{1/n}$)	7.9448	11.1472	11.3811	8.2996
	n_F	4.3941	4.4095	4.5772	4.2151
	R^2	0.7740	0.6952	0.6354	0.5975
	ARE	7.3137	31.0758	21.7025	21.7442
Sips	Q_m (mg g^{-1})	37.24	43.51	48.46	41.55
	K_S (L mg^{-1})	0.0208	0.0365	0.0530	0.0520
	M	0.4237	0.4635	0.2768	0.3791
	R^2	0.9659	0.9849	0.9859	0.9906
	ARE	2.6981	1.2530	3.4722	13.2478
Redlich-Peterson	A_{RP}	0.5464	1.2330	1.6957	1.0791
	B_{RP}	0.0025	1.0057	0.0068	0.0046
	G	1.2455	0.0045	1.2395	1.2322
	R^2	0.9598	0.9630	0.9399	0.9325
	ARE	2.2143	8.2172	5.7629	34.8463
Jovanovich	Q_m (mg g^{-1})	37.35	44.00	49.53	43.83
	K_J	0.0163	0.0253	0.0387	0.0283
	R^2	0.9615	0.9629	0.9355	0.9241
	ARE	2.1505	8.9188	6.5416	38.2674
Dubinin-Radushkevich	Q_m (mg g^{-1})	36.51	42.97	49.46	40.89
	b_{DR} (mol^2 kJ^{-2})	0.0002	0.0000872	0.0000387	0.0000368
	E_{ads} (kJ mol^{-1})	50.00	75.73	113.60	122.53
	R^2	0.9502	0.9626	0.9730	0.9862
	ARE	3.0045	3.1859	3.5685	7.5640

The experimental data were adjusted to the Sips model, and results allow to infer that adsorption occurred on a heterogeneous surface in which the energetic distribution of the adsorption sites is verified.

Results were obtained from the analysis of the coefficient of determination (R^2) and from the average relative error. In this sense, the choice of the Sips model isotherm was based on the comparison of such parameters according to what was described in Table 6.

The mean energy of adsorption represents the energy released during the adsorption process. The E_{ads} value from 1 to 8 kJ mol^{-1} indicates physisorption, from 8 to 16 kJ mol^{-1}, it indicates ionic exchange and the E_{ads} value higher than 20 kJ mol^{-1} indicates a chemical adsorption (Oyango et al., 2006; Tahir and Rauf, 2004). The values corresponding to 50.00 kJ mol^{-1}, 75.73 kJ mol^{-1}, 113.60 kJ mol^{-1}, and 122.53 kJ, for the respective samples: NK, KA-01, KA-02 and KA-05, indicate that etheramine adsorption in the treated kaolinite involves the mechanism of chemisorption.

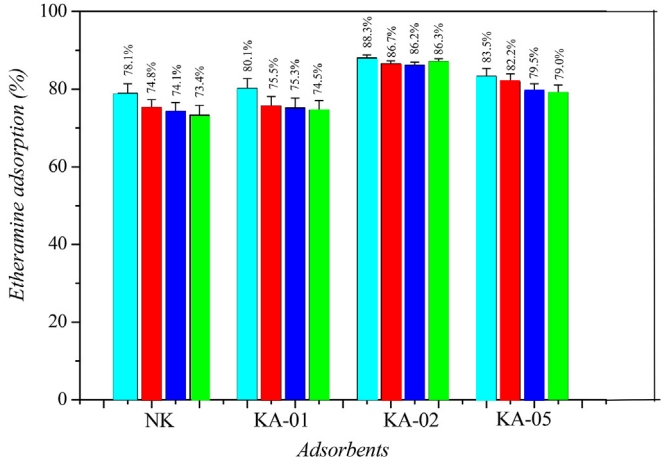

Fig. 7. Reuse tests.

3.6. Reuse test

Regeneration of the adsorbent is an important factor for the economic viability of its use. In this sense, the used adsorbents underwent three reuse tests and the results are shown in Fig. 7. There was a slightly significant decrease in the efficiency of adsorption. Such results are in accordance with the literature (Unuabonah et al., 2008; Jin et al., 2014; Guo et al., 2011; Guerra and Silva, 2014). It was possible to observe that the proposed desorption methodology was efficient. Furthermore, the desorbed adsorbate may be reused in the flotation step, which makes the process economically viable.

The comparative analysis of etheramine adsorption in the different adsorbents after each use was accompanied by ATR and results are shown in Fig. 8. The etheramine used in the iron ore processing under operational conditions of pH = 10 has a molecular structure that corresponds to R-O–$(CH_2)_3$–NH_2, and in the ionic form, R-O–$(CH_2)_3$–NH_3^+. Therefore, in the infrared spectra of etheramine the bands of 2967 and 2864 cm^{-1} are attributed to the vibrations of axial deformation of hydrogen atoms bonded to methyl groups. Adsorption in the region of 2300 and between 1590 and 1550 cm^{-1} are associated with angular deformations of NH_2. The region between 1500 and 600 cm^{-1} is associated to several types of vibrations: axial and angular deformations of C–O, C–N and C–C bonds. The band at 1477 cm^{-1} is related to the angular deformation of $(CH_2)_3$, and the band at 1119 cm^{-1} refers to the axial deformation of C–O in aliphatic ethers.

By comparing the spectra of etheramine and kaolinites, both natural and modified, it was possible to verify the appearance of bands located at 2967 cm^{-1} and 2864 cm^{-1} in the kaolinites after adsorption, which are characteristics of etheramine, and validates the adsorption of etheramine. By analyzing the spectra of reuse, it is possible to observe that there were no significant changes in the

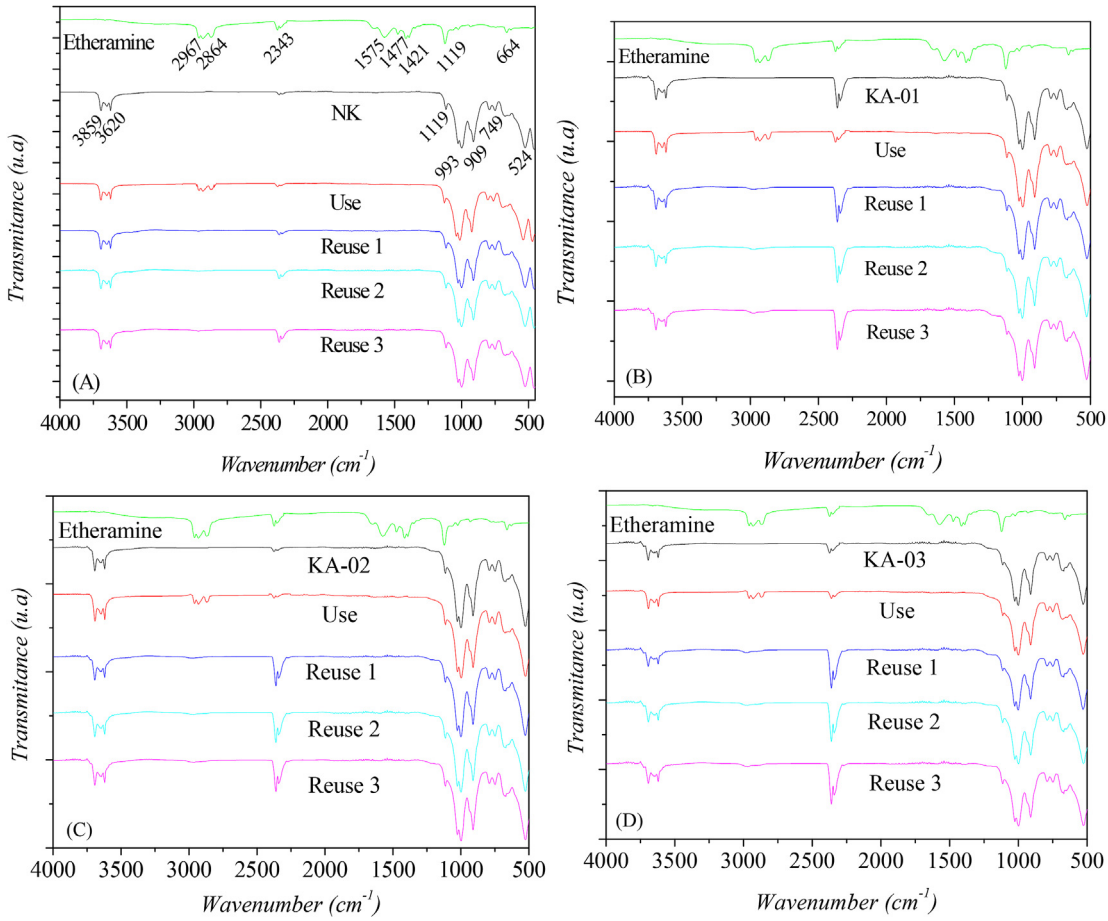

Fig. 8. FTIR spectra of etheramine, adsorbent (fresh and reused): NK (A), KA-1 (B), KA-2 (C) and KA-5 (D).

intensity of the band as kaolinite was reused.

4. Conclusions

The acid treatments caused changes in the chemical composition and textural properties of kaolinite. The time at which equilibrium was reached was close to 30 min for all the adsorbents. After comparing the etheramine adsorption kinetics, it was possible to observe that the efficiency of etheramine removal in KA-02 improved significantly, while for the samples KA-01 and KA-05 it was similar to the efficiency of etheramine removal in NK samples. The adjustment of experimental data of the kinetic models revealed that data were better described by the pseudo-second order model. The adsorption isotherm results showed that the data adjusted to the Sips model, and the E_{ads} value indicates that adsorption involved a chemisorption process. Regarding the reuse tests, it was possible to observe a not so significant decrease in the efficiency of removal as the adsorbents were reused. Then, it was possible to confirm that the kaolinite modified applying the three treatments (with KA-02 standing out) may be a good alternative for etheramine adsorption since it is a low-cost material and presents a considerable removal efficiency even after reuse.

Acknowledgements

The authors thank CAPES, FAPEMIG and CNPq for the financial support; LGRQ/UFLA, where the experiments were conducted; and the Department of Mining Engineering/UFMG for the XRD, zeta potential and surface area analyses.

Appendix A. Supplementary data

Supplementary data related to this article can be found at http://dx.doi.org/10.1016/j.jenvman.2017.04.003.

References

Araújo, D.M., Yoshida, M.I., Takahashi, J.A., Carvalho, C.F., Stapelfeldt, F., 2010. Biodegradation studies on fatty amines used for reverse flotation of iron ore. Int. Biodeterior. Biodegr. 64, 151–155.

Asadollahzadeh, M., Tavakoli, H., Mostaedi, M.T., Hosseini, G., Hemmati, A., 2014. Response surface methodology based on central composite design as achemometric tool for optimization of dispersive-solidification liquid–liquid microextraction for speciation of inorganic arsenic in environmental water samples. Talanta 123, 25–31.

Chatterjee, S., Kumar, A., Basu, S., Dutta, S., 2012. Application of response surface-methodology for methylene blue dye removal from aqueous solution using lowcost adsorbent. Chem. Eng. J. 181–182, 289–299.

Chen, Y., Lu, D., 2015. CO_2 capture by kaolinite and its adsorption mechanism. Appl. Clay Sci. 104, 221–228.

Cristóbal, A.G.S., Castelló, R., Luengo, M.A.M., Viscayno, C., 2009. Acid activation of mechanically and thermally modified kaolins. Mater. Res. Bull. 44, 2103e2111.

Dudkin, B.N., 2010. Mechanical activation of kaolinite in the presence of aluminumsulfate. Russ. J. Appl. Chem. 83, 1077e1079.

Filippov, L.O., Severov, V.V., Filippova, I.V., 2014. An overview of the beneficiation of iron ores via reverse cationic flotation. Int. J. Miner. Process. 127, 62–69.

Frontistis, Z., Antonopoulou, M., Petala, A., Venieri, D., Konstantinou, I., Kondarides, D.I., Mantzavinos, D., 2017. Photodegradation of ethyl paraben using simulated solar radiation and Ag_3PO_4 photocatalyst. J. Hazard. Mater. 323, 478–488.

Garg, U.K., Kaur, M.P., Sud, D., 2008. Removal of nickel (II) from aqueous solution by adsorption on agricultural waste biomass using a response surface

methodological approach. Bioresour. Technol. 99, 1325–1341.
Guerra, D.J.L., Silva, R.A.R., 2014. Kinetic and thermodynamic studies of Brazilian illite-kaolinite in natural and intercalated forms as adsorbents to removal of Zn^{+2} from aqueous solutions. J. Taiwan Inst. Chem. Eng. 45, 268–274.
Guo, W., Hu, W., Pan, J., Zhou, H., Guan, W., Wang, X., Dai, J., Xu, L., 2011. Selective adsoption and separation of BPA from aqueous solution using novel molecularly imprinted polymers based on kaolinite/Fe_3O_4 composites. Chem. Eng. J. 171, 603–611.
Hammed, B.H., Tan, I.A.W., Ahmad, A.L., 2008. Adsorption isotherm Kinect modeling and mechanism of 2, 4, 6- triclorofenol on coconut husk – based activated carbon. Chem. Eng. J. 144, 235–244.
Ho, Y.S., Mckay, G., 1999. Pseudo-second order model for sorption process. Process. Biochem. 34, 19451–19465.
Jin, X., Jiang, M., Du, J., Chen, Z., 2014. Removal of Cr (VI) from aqueous solution by surfactant-modified kaolinite. J. Indus. Eng. Chem. 20, 3025–3032.
Kavalathy, H.-M., Requpathi, I., Pillai, M.-G., Miranda, L.-R., 2009. Modelling, analysis and adsorption parameters for H_3PO_4 activated rubber wood sawdust using surface methodology (RSM). Colloids Surfaces B Biointerfaces 70, 35–45.
Khawmee, K., Suddhiprakam, A., Kheoruenromne, I., Singh, B., 2013. Surface charge properties of kaolinite from Thai soils, 192, 120–131.
Komadel, P., Mandejová, J., 2012. Changes in layer charge of clay minerals upon acid treatment as obtained from their interactions with methylene blue. Appl. Clay Sci. 55, 100–107.
Lagergren, S., 1898. About the theory of so-called adsorption of soluble substances. K. Sven. Vetenskapsakad. Handl. 24, 1–39.
Ma, X., Marques, M., Gontijo, C., 2011. Comparative studies of reverse cationic/anionic flotation of Vale iron ore. Int. J. Miner. Process. 100, 179–183.
Magriotis, Z.M., Leal, P.V.B., Sales, P.F., Papini, R.M., Viana, P.R.M., 2010. Adsorption of etheramine on kaolinite: a cheap alternative for the treatment of mining effluents. J. Hazard. Mater. 184, 465–471.
Magriotis, Z.M., Sales, P.F., Ramalho, T.C., Rocha, M.V.J., Leal, P.V.B., 2013. Influence of pH and of the interactions involved in etheramine removal in kaolinite: insights about adsorption mechanism. J. Phys. Chem. C 117, 21788–21794.
Melo, J.D.D., Costa, T.C.C., Medeiros, A.M., Paskocimas, C.A., 2010. Effects of thermal and chemical treatments on physical properties of kaolinite. Ceram. Int. 36, 33–38.
Morsy, F.A., EL-Sherbiny, S., Hassan, M.S., Mohammed, H.F., 2014. Modification and evaluation of Egyptian kaolinite as pigment for paper coating. Powder Technol. 264, 430–438.
Mudd, G.M., 2010. The environmental sustainability of mining in Australia: key mega-trends and looming constraints. Resour. Policy 35, 98–115.
Ndlovu, B., Farrokhpay, S., Forbes, E., Bradshaw, D., 2015. Characterization of kaolinite colloidal and flow behavior via crystallinity measurements. Powder Technol. 269, 505–512.
Nunes, C.A., Freitas, M.P., Pinheiro, A.C.M., Bastos, S.C., 2012. Chemoface: anovel free user-friendly interface for chemometrics. J. Braz. Chem. Soc. 23, 2003–2010.
Oyango, M.S., Kojima, Y., Aoyi, O., Bernardo, E.C., Matsuda, H., 2006. Adsorption equilibrium modeling and solution chemistry dependence of fluoride removal from water by trivalente-cation-exchange zeolite F-9. J. Colloid Interface Sci. 279, 341–350.
Panda, A.K., Mishra, B.G., Mishra, D.K., Singh, R.K., 2010. Effect of sulphuric acid treatment on the physic-chemical characteristics of kaolin clay, 363, 98–104.
Perez, A., Montes, M., Molina, R., Moreno, S., 2014. Modified clays as catalysts for the catalytic oxidation of ethanol. Appl. Clay Sci. 95, 18–24.
Poonkuzhali, K., Rajeswari, V., Saravanakumar, T., Viswanathamurthi, P., Park, S.M., Govarthanan, M., Sathishkumar, P., 2014. Reduction of hexavalent chromium using Aervalanata L.: elucidation of reduction mechanism and identification of active principles. J. Hazard. Mater. 272, 89–95.
Ravikumar, K., Ramalingam, S., Krishnan, S., Balu, K., 2006. Application of response surface methodology to optimize the process variables for reactive red and acid brown dye removal using a novel adsorbent. Dyes Pigments 70, 18–26.
Sales, P.F., Magriotis, Z.M., Rossi, M.A.L.S., Resende, R.F., Nunes, C.A., 2013. Optimization by response surfasse methodology of the adsorption of coomassie blue dye on the natural and acid-treated clays. J. Environ. Manage. 130, 417–428.
Singh, K.P., Gupta, S., Singh, A.K., Sinha, S., 2011. Optimizing adsorption of crystalviolet dye from water by magnetic nanocomposite using response surface-modeling approach. J. Hazard. Mater. 186, 1462–1473.
Tahir, S.S., Rauf, N., 2004. Removal of a cationic dye from aqueous solutions by adsorption onto bentonite clay. Chemosphere 63, 1842–1848.
Tarley, C.R.T., Silveira, G., Santos, W.N.L., Matos, G.D., Silva, E.G.P., Bezerra, M.A., Miro, M., Ferreira, L.C.F., 2009. Chemometric tools in electroanalytical chemistry: methods for optimization based on factorial design and response surface methodology. Microchem. J. 92, 58–67.
Ugochukwu, U., Jones, M.D., Head, I.M., Manning, D.A.C., Fialips, C.I., 2014. Effect of acid activated clay minerals on biodegradation of crude oil hydrocarbons. Int. Biodeterior. Biodegradation 88, 185–191.
Unuabonah, E.I., Adebowale, K.O., Dawodu, F.A., 2008. Equilibrium, kinetic and sorber design studies on the adsorption of aniline blue dye by sodium tetraborate-modified kaolinite clay adsorbent. J. Hazard. Mater. 157, 397–409.
Vargas, A.M.M., Cazetta, A.L., Martins, A.C., Moraes, J.C.G., Garcia, E.E., Gauze, G.F., Costa, W.F., Almeida, V.C., 2012. Kinetic and equilibrium studies: adsorption of food dyes acid yellow 6, acid yellow 23, and acid red 18 on activated carbon from flamboyant pods. Chem. Eng. J. 181/182, 243–250.
Wei, S., Tan, W., Liu, F., Zhao, W., Weng, L., 2014. Surface properties and phosphate adsorption of binary systems containing goethite and kaolinite. Geoderma 213, 478–484.
Xu, H., Jin, X., Chen, P., Shao, G., Wang, H., Chen, D., Lu, H., Zhang, R., 2015. Preparation of kaolinite nanotubes by a solvothermal method. Ceram. Int. 41, 6463–6469.
Yuan, G.D., Theng, B.K.G., Churchman, G.J., Gates, W.P., 2013. Chapter 5.1-clays and clay minerals for pollution control. Developments in clay science. 5, 587–644.